Microwave Reflectometry Sensing System For Low-Cost In-Vivo Skin Cancer Diagnostics

Raissa Schiavoni
University of Salento
Gennaro Maietta
Local Health Unit of Lecce
Elisabetta Filieri
Local Health Unit of Lecce
Andrea Cataldo (andrea.cataldo@unisalento.it)
University of Salento

Research Article

Keywords:

Posted Date: March 11th, 2022

DOI: https://doi.org/10.21203/rs.3.rs-1320222/v1

Microwave reflectometry sensing system for low-cost in-vivo skin cancer diagnostics

Raissa Schiavoni[1], Gennaro Maietta[2], Elisabetta Filieri[2], and Andrea Cataldo[1,*]

[1]University of Salento, Department of Engineering for Innovation, Lecce, 73100, Italy
[2]Local Health Unit of Lecce, Italy
[*]andrea.cataldo@unisalento.it

ABSTRACT

Skin cancer is one of the most commonly diffused cancer in the world and its incidence rates have constantly increased in recent years. At the current state of the art, there is a lack of objective, quick and non-invasive methods for diagnosing this condition; this, combined with hospital crowding, may lead to late diagnosis. Starting from these considerations, this paper addresses the implementation of a microwave reflectometry based-system that can be used as a non-invasive method for the in-vivo diagnosis and early detection of biological abnormalities, such as skin cancer. This system relies on the dielectric contrasts existing between normal and anomalous skin tissues at microwave frequencies. In particular, a truncated open-ended coaxial probe was designed, manufactured and tested to sense (in combination with a miniaturized Vector Network Analyzer) the variations of skin dielectric properties on a group of volunteer patients. The specific data processing demonstrated the suitability of the system for discriminating malignant and benign lesions from healthy skin, ensuring simultaneously effectiveness, low cost, compactness, comfortability and high sensitivity.

Introduction

The Skin Cancer Foundation estimates that in the U.S., more than 9.500 people are diagnosed with skin cancer every day and more than two people die of the disease every hour, according to data collected in the year 2022 [1]. Skin cancer, in fact, is the most common type of cancer and a large number of tumour types can affect the skin, which is the human body's largest organ [2]. The most common skin cancers, apart from melanoma, are basal cell carcinoma (BCC) [3; 4; 5], squamous cell carcinoma (SCC) [6; 7] and epithelioma. An early diagnosis is the key to guarantee the possibility of full recovery and to prevent the tumour from penetrating further into the underlying tissues causing metastasis. These skin cancers only rarely cause symptoms in the early stages and it becomes difficult to be detected quickly; as a result, prevention becomes crucial. However, currently there is a lack of objective non-invasive methods for the characterization of skin lesions and the related diagnosis, that can ensure simultaneously an in-vivo modality, large use possibility and low-cost instrumentation. As a matter of fact, when some suspicious cases occur, typically, the dermatologist performs a visual examination of the skin through epiluminescence [8]. Nevertheless, this technique strongly depends on the Clinician's subjective experience and may suffer from low clinical accuracy. Furthermore, a definite diagnosis of cancer can be made only after a biopsy [9; 10], which is an invasive procedure involving the removal of a portion of tissue and, consequently, the analysis with a microscope. Because of the high error probability deriving from the dermatologist exams, biopsies are requested very frequently, even for portions of skin that are actually healthy, causing discomfort and concern to the patients. On such basis, it goes without saying that, in the perspective of the so-called Health 4.0 Era [11; 12], the development of advanced digital technologies, new systems and wearable devices play a crucial role in improving healthcare through periodical screening, diagnosis and treatment of cancers. To these purposes, a non-invasive, portable, low-cost, microwave reflectometry-based system was developed for analysing in-vivo suspicious skin lesions. The proposed methodology is based on the detection of the dielectric contrast between healthy and anomalous skin tissues at microwaves. As detailed in the following, a truncated open-ended coaxial probe was designed, manufactured and tested to sense (in combination with a miniaturized Vector Network Analyzer) the variations of skin dielectric properties on a group of

volunteer patients. The proposed sensing system has the twofold purpose of i) detecting early-stage cancer; and of ii) monitoring the healing phase and the evolution in time of cutaneous areas which were subjected to surgeries after cancers. With regard to the early-stage detection, the proposed system allows to improve the diagnostic accuracy supporting the clinical personnel in making a more objective diagnosis together with the possibility of optimizing the requests of costly and invasive biopsies. As for the monitoring of the post-surgery phase, the proposed system would allow the possibility of a periodic control of the tissue status associated to its corresponding dielectric response, which can be regarded as an effective precautionary measure for avoiding recurrences.

This paper is organized as follows. First, Section 1 addresses the motivations of the work and provides an overview of state-of-the-art solutions for monitoring and diagnosis of skin cancers. Section 2 describes the basic theoretical background behind the proposed system. Section 3 presents the design, the optimization and the characterization of the non-invasive coaxial probe. Section 4 describes the experimental measurement setup, the procedure for extrapolating the dielectric properties of skin tissues from the reflectometric measurements and the investigative campaign on people and voluntary patients. Section 4 reports the experimental results together with the statistical analysis performed on the data. Finally, conclusions and future work are outlined in Section 5.

1 Review of the State Of The Art and Motivation of the Present Work

As briefly discussed in the Section , in the literature, most works relate to different methodologies for skin cancer detection ranging from optical, photodynamic, sonography, thermal imaging, and electromagnetic. More in detail, confocal Raman spectroscopy performs the analysis of the light that is scattered by the tissue; this, however, requires very costly instrumentation [13]. Similarly, methods such as near-IR [14] or Terahertz spectroscopy [15] involve expensive equipment. Other technologies are based on thermography which analyze the temperature of the skin or lesion surface from the intensity of emitted infrared radiation [16]. Also this method needs expensive instrumentation and, in addition, it is widely affected by external noise. Bio-electrical impedance or Optical Coherence Tomography (OCT) may be affected by low measurement accuracy and they are both significantly influenced by physiological or environmental variations. Considering the aforementioned limitations, the proposed system exploits microwave reflectometry, combining the requirements of (i) low cost, (ii) compactness, (iii) quick response time, (iv) comfortability (no biopsy) and (v) high sensitivity. More specifically, this technique is particularly sensitive to the different dielectric properties between normal skin and lesions. As a matter of fact, cancer tissue differs in composition with respect to healthy tissue from which the cancer originated. Some of the factors that contribute to these variations include increased vasculation and blood content [17], differences in protein and mineral content [18] as well as differences in the water content or water distribution and structure, e.g., whether the water is free or bound. This means that it is extremely important to perform in-vivo diagnostics, in order to preserve the physical and chemical composition of suspect tissues. In fact, it is important to underline that, when excised, the tissues under test present some differences in characteristics with respect to the original in-vivo status, due to different conditions such as the temperature, the loss of tissue water content after excision and the absence of blood circulation. In this regard, an additional applicative limitation of most of the state-of-the-art techniques related to the necessity of analysing of portions of tissues excised through biopsies [19; 20; 21], thus altering the intrinsic properties of the tissues. As a consequence, the final results on the discrimination of skin cancers are ambiguous and some substantial discrepancies are also observed among the data presented in different publications. These limitations motivate the development of systems capable of discriminating, directly in vivo, the significant dielectric variations of skin tissues associable to suspicious or malignant tumour cases at their very early stage, by comparing their dielectric response with reference healthy areas. Another limitation of the methods based on dielectric detection existing at the current state of the art relies to the analysis usually conducted at a single frequency [22]. As well known, the complex dielectric permittivity of biological tissues depends strongly on the frequency and, as a consequence, a single-frequency analysis can give a very limited information. Moreover, as further consideration, operating in a lower frequency range implies significant advantages in terms of reduced costs and portability of equipment. Another aspect motivating the present work relates to the possibility of diagnosing tumours at their earliest stage. In fact, if not diagnosed suddenly, skin cancers can grow into nearby areas and they

can invade and slowly destroy the surrounding tissues, as illustrated in Figure 1, provoking serious consequences that ultimately can lead to death.

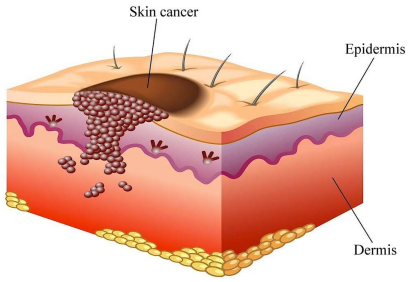

Figure 1. Growth of a skin cancer. © Howcast

In addition, knowing the dielectric signature of a body's portion can be critically important for several aspects beyond cancer diagnostics. It is worth noting that even when the treatment of a carcinoma was successfully terminated, there is a residual possibility of a recurrence [23]. In perspective of prevention measures, there is a need to monitor the dielectric variations of the skin area at risk in order to detect abnormalities in time. Viable tools for large scale prevention monitoring could be useful also for several people such as workers frequently exposed to the sun [24] as well as other with risk factors including: genetic predisposition [25; 26; 27], age [28], light skin, hair, and eye pigmentation [29], geographic position [30; 31; 32], fragile immune system [33] exposure to other radiation or to certain chemicals, chronic inflammatory skin conditions and complications of burns, scarring, or infections [34; 35]. On the basis of all the aforementioned aspects, the present work aims at proposing an alternative system which can detect suspicious or anomalous lesions directly in vivo and, at the same time, in perspective of prevention, it can be applied for large-scale monitoring activity of skin dielectric characteristics thus alerting when suspect variations occur. For the sake of assessing the proposed method, in this paper, investigations were conducted on some voluntary patients presenting different kind of skin lesions which were preliminarily diagnosed by the standard so-called ABCDE visual analysis [36; 37].

2 Theoretical Background

Microwave reflectometry (MR) is a powerful tool for several monitoring and diagnostic applications [38; 39; 40; 41; 42; 43; 44; 45]. Typically, in MR, an electromagnetic test signal is propagated through a sensing element. As a result of the electromagnetic interaction, the incident signal is reflected back and it carries significant information which can be directly associated to dielectric properties of the system under test. Because microwaves are non-ionizing radiation, they are suitable for diagnostic in-vivo applications on biological tissues, such as in the case of early-stage detection of skin cancer. As reported in the state of the art, the dielectric properties of cancer tissue differ from healthy tissue, mostly because of the different water and protein content [46; 47; 48]. This difference can be detected by microwave-based systems.

More specifically, the dielectric properties of biological tissues can be described in terms of frequency-dependent complex dielectric permittivity $\varepsilon^*(f)$, according to the following equation 1

$$\varepsilon^*(f) = \varepsilon'(f) - j\varepsilon''(f) \tag{1}$$

where ε' is the relative dielectric constant, ε'' is the relative dielectric loss factor and f is the frequency [49]. For brevity, hereon the term "relative" is assumed and omitted in the text. Biological tissues exhibit considerable inhomogeneities, caused by several factors such as the nature, structure, and organization of the cellular components. Therefore, at the state of the art, different dielectric models are available describing the frequency dependent complex permittivity, such as the Cole-Cole model [50; 51].

The dielectric contrast between cancerous and healthy tissues provokes a different interaction with microwaves thus allowing the correspondent characteristic detection. In fact, the dielectric characteristic is directly associated to

the reflected signal, and it can be revealed in terms of the frequency-dependent reflection scattering parameter $S_{11}(f)$ of the probe when this is in contact with the biological tissue. Generally, the $S_{11}(f)$ measurements can be obtained through a Vector Network Analyzer (VNA) connected to a probe which can be inserted in or in contact with the system under test. For the sake of ensuring in-vivo and non-invasive measurements, a suitable probe configuration is that of a truncated open ended coaxial probe which when in contact with the tissue sample under test can be sensible to the dielectric variations. To this purpose, it can be exploited the so-called fringing effect associated to a termination flange of the truncated coaxial probe [52]. In Figure 2 it is schematized the equivalent electrical circuit of the probe termination associated to the capacitive fringing effect, where C_f and C_0 are the internal and external fringing capacitances, respectively, ε^* is the complex permittivity of the material under test (MUT) in contact with the probe and Z_0 is the characteristic impedance of the coaxial probe.

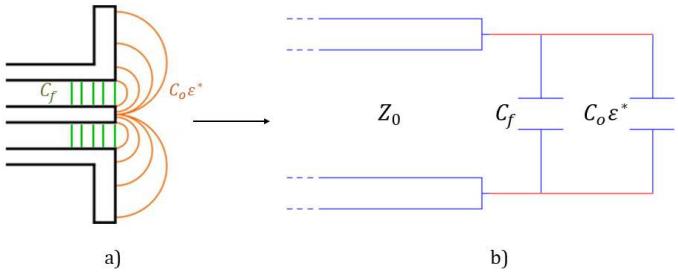

Figure 2. Cross-section of an open-ended coaxial probe **a)**, equivalent lumped-element electric circuit **b)**

From the theory [52] the equation that relates the $\varepsilon^*(f)$ to the corresponding scattering parameter of the MUT, $S_{11,MUT}(f)$ measured in correspondence of the calibration plane reported in Figure 2, is given by the following equation:

$$\varepsilon^* = \frac{1 - S_{11,MUT}(f))}{j\omega Z_0 C_0 \left[1 + S_{11,MUT}(f)\right]} - \frac{C_f}{C_0} \tag{2}$$

where ω is the angular frequency and $j^2 = -1$ is the complex imaginary unit. Typically, this technique is implemented in commercially available software and probes but, in view of the specific purposes of the present application, there is the need to use customized probes together with a dedicated algorithm, as detailed in Section 4.

3 Probe Design and Simulations

Considering the requirements of non-invasiveness and surface skin contact, the aforementioned open-ended coaxial probe configuration was chosen. Through the use of the CST Microwave Studio software, a preliminary simulation analysis was performed to identify the most suitable probe geometry. To this purpose and to predict the electromagnetic interaction of the probe on the skin surface, the biological tissue has been modelled through a three-layer structure composed by skin, fat and muscle. More specifically, the skin layer includes the stratum corneum, the epidermis and the dermis. The dielectric parameters of biological tissues have been superimposed by the reference values available in the "Gabriel&Gabriel" database [53]. For the sake of optimizing the probe configuration in terms of dielectric sensitivity, some recurrent parametric simulations have been implemented in order to guarantee good response in the frequency range of interest (which is in the order of few GHz) and to ensure a good spatial resolution in the sensing volume in the subsurface skin region potentially affected by tumoral pathologies. As well known, the penetration depth of a coaxial probe is proportional to its diameter; hence, as a general requirement, the smaller the diameter, the higher will be the sensitivity related to the skin layer in which the tumour initially originates. On the other hand, if the stratum corneum layer is relatively thick, it may happen that epidermis and dermis layers are not sufficiently sensitive to the electromagnetic (EM) field. As a consequence, a good trade-off between the geometric probe configuration and the depth penetration sensitivity must be obtained. Considering these requirements, the parametric simulations allow to achieve an optimal probe configuration as detailed in Figure 3. In

particular, the outer diameter of the inner conductor is 1.25 mm, the inner diameter of the outer conductor is 4.2 mm and the dielectric material between the two conductors is Teflon. The probe, having an external length of 11 mm, is equipped with an external metallic flange (i.e., a ground plane), with a diameter of 17.2 mm, in order to enhance its sensitivity in terms of the fringing field effect, described in Section 2.

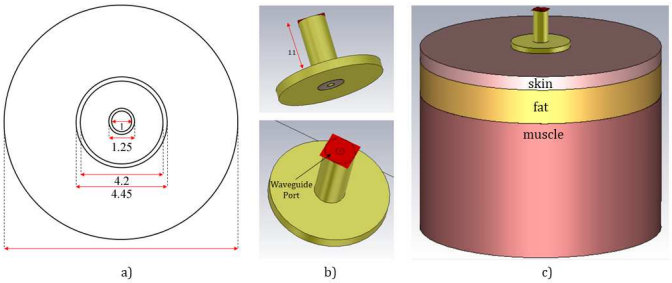

Figure 3. Scheme of the simulated system: Bottom view of the probe and geometric dimensions in mm **a)**, Perspective view of the probe **b)**, Probe in contact with the three-layer modelled biological tissue **c)**.

After this preliminary design phase, additional simulations were performed in order to evaluate the response for different thickness of the skin layer so as to cover the variability range of different parts of the body. In this regard, it is known that, typically the skin varies from 0.5 mm thick (generally only on the eyelids) to 4 mm [54]. As can be seen in Figure 4, which shows the $S_{11}(f)$ response in function of the skin thickness, the overall behaviour is not substantially influenced by this parameter. As a consequence, the designed probe configuration can be applied in different parts of the body.

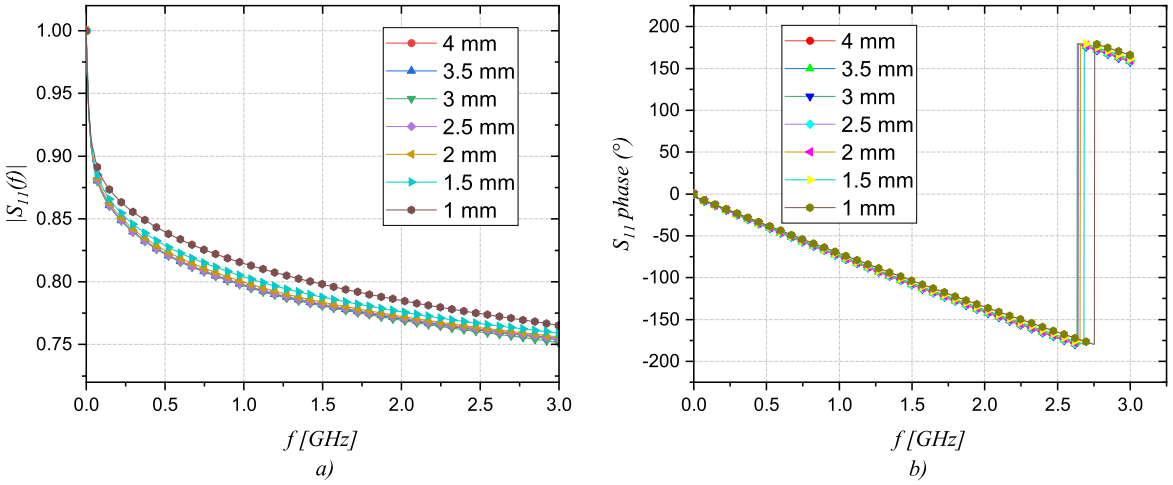

Figure 4. Simulated scattering parameter in function of the skin thickness. Magnitude response **a)**, Phase response **b)**

Figure 5 shows the simulation results of the electric field penetration for three different skin thickness, in order to evaluate the deep penetration of the EM field in terms of sensing capability.

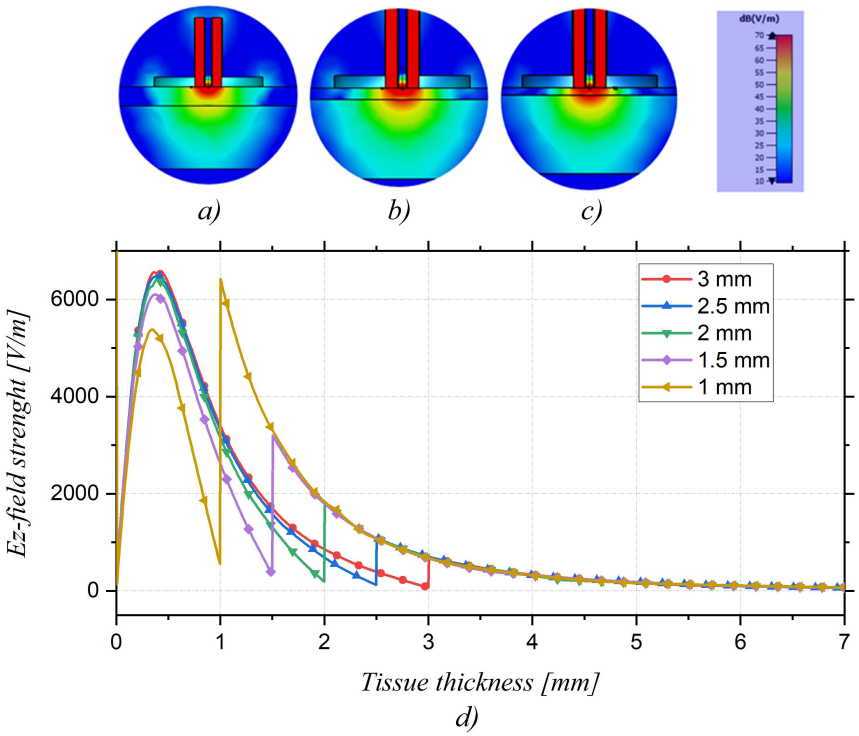

Figure 5. Simulation results of E-field at different skin thickness: 3 mm **a)**, 2mm **b)**, 1 mm **c)**. Ez-field strength as a function of tissue thickness **d)**

As can be seen from Figure 5 b), for the all different simulated skin thickness, a distinct peak of the electric field is observed in the skin region. At the interface between the skin and fat layer, as expected, due to their corresponding different dielectric values, a significant field variation occurs, according to the following equation:

$$E_1\varepsilon_1 = E_2\varepsilon_2 \tag{3}$$

where ε_1 and ε_2 represent the dielectric permittivity of skin and fat while E_1 and E_2 the normal component values of the electric field in skin and fat respectively. The graph shows that after about 3 mm the effect of the field can be considered negligible; therefore the detection depth of the probe is about 3 mm, according to the application purpose.

4 Materials and Methods

As explained in the previous sections, the detection procedure involves the initial measurements of the $|S_{11}(f)|$. In view of the practical application, which involves low-cost and compact equipment suitable for portable (or wearable) approach, a miniaturized Vector Network Analyzer (m-VNA) developed by HCXQS (commercially available with the name of nanoVNA) has been chosen. The m-VNA is a compact (dimensions 15 cm x 10 cm x 6 cm), low-cost (about 100 euros) VNA with an operating frequency range 50 kHz-3 GHz. For the sake of assessing the metrological performance a comparative analysis between the m-VNA and a reference benchtop accurate instrument (i.e. VNA R&S ZLV6) was preliminary conducted; as a result, the measurement deviation in terms of root mean square error (RMSE) is 0.0135.

After the preliminary validation activity, a specific investigation campaign was conducted involving voluntary people. The experiments were carried out on volunteer subjects who signed an informed consent, containing the consent to use and share the anonymized data for scientific publication, and regarding the harmlessness of the system and the acknowledgement that the system does not lead to any permanent or temporary alteration whatsoever.

The study was conducted according to the guidelines of the Declaration of Helsinki [55]. The Ethic Committee "Comitato Etico ASL/LE" of the Local Health Authority of Lecce (Italy) has in charge the documentation describing the specific protocol activity. The test cases considered in the investigative campaign can be grouped into three major categories: (i) moles that can be regarded as pigmented skin healthy lesions slightly differing from the adjacent normal skin, (ii) malignant and (iii) benign tumours. A group of 11 informed volunteers participated in the research campaign which was conducted with the clinical supervision of the medical personnel who performed the tests and, for each case, diagnosed possible pathologies (i.e. both malignant and benign tumours) through the standard so-called ABCDE visual analysis and epiluminescence. Table 1 summarizes the details of all the analysed cases, also indicating the related body parts and the corresponding dermatological diagnosis. As reported in Table 1, 4 subjects were affected by malignant lesions (two basal cell carcinoma BCC and two epitheliomas), 2 presented benign lesions (keratosis) and, finally, 5 had normal moles.

Table 1. Characteristics and typologies of the 11 considered test-cases of the voluntary subjects participating in the campaign

Subject number	Diagnosis
#1	Mole
#2	Mole
#3	Mole
#4	Mole
#5	Mole
#6	Malignant tumour (BCC)
#7	Malignant tumour (BCC)
#8	Malignant tumour (epithelioma)
#9	Malignant tumour (epithelioma)
#10	Benign tumour (keratosis)
#11	Benign tumour (keratosis)

For each test-case under examination, the adopted in-vivo protocol consisted of a double test; firstly, the suspected area affected by lesion was investigated and, subsequently, the normal skin area in the near proximity of the lesions was also analysed for the sake of comparison. Experiments were carried out by connecting the designed probe to the m-VNA and the raw data was acquired on a PC. Figure 6 shows the used setup highlighting the contact between the skin surface and the probe that, in the current prototypal version of the system, was just pressed manually on the skin tissue to ensure a very stable contact. It should be mentioned that, although the measured response already showed good repeatability, it is envisaged that the probe will be inserted in a wearable flexible structure equipped with a miniaturized strength sensor thus enabling a stable contact between skin and probe.

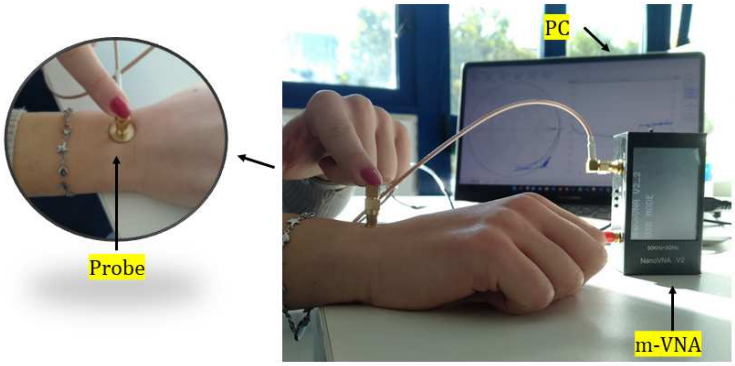

Figure 6. Experimental setup highlighting the contact between the skin surface and the probe

In order to extrapolate the frequency-dependent dielectric permittivity from the $S_{11}(f)$ measurements, according to the theoretical background described in Section 2, a specific algorithm was implemented in LabVIEW, as reported in [56]. More in detail, the extrapolation procedure can be applied for customized coaxial probe, avoiding the complete characterization of the probe capacitance, reported in equation 2. The procedure, which is described in detail in [56], also implements a specific calibration procedure suitable for the specific probe flange configuration. Three preliminary calibration measurements have to be performed on well-referenced dielectric samples (i.e. air, acetone and isopropyl alcohol) thus allowing compensating for systematic errors and parasitic effect introduced by the setup.

Experimental Results

As aforementioned, the experimental measurements were carried out on the 11 volunteer patients, as categorised: moles, malignant tumours and benign tumours. The measurements results are reported in Figure 7 which shows, for each test-case the comparison between the magnitude of the scattering parameter as acquired from lesions (moles or tumours) and the corresponding normal skin, respectively.

As a first observation, it can be noticed that, over the whole considered frequency range, the tumour cases exhibit different values with respect to the moles. The response of moles is systematically lower than that corresponding healthy skin portion, while as for the tumour cases an opposite trend is observed. This preliminary result suggests that the system is capable to discriminate accurately between moles, normal skin and tumours. Additionally, considering the tumours cases, the difference between the responses of benign tumours and healthy skin is more significant. A similar trend was also observed for the phase response of $S_{11}(f)$, not reported for the sake of brevity. As described in Section 4, from the measured $S_{11}(f)$ data, it is possible to extrapolate the complex permittivity spectrum thus characterizing the specific dielectric signature of the sample. Figure 8 shows the obtained results which refer to the 250 MHz-3 GHz frequency range.

As can be easily seen in Figure 8, the four tissues categories exhibit different dielectric characteristics. Regarding the skin lesions, it is possible to identify three groups of curves: benign tissues (keratosis) which show the lowest permittivity values, malignant tissues (basal cell carcinoma and epithelioma) which shows the intermediate values and moles which present the highest values of permittivity. The described trend is the same for both the real and the imaginary part of the complex permittivity. The observed trend indicates that the complex permittivity progressively decreases as the tissue degenerates from normal to tumoral condition.

To further analyse the data and also in view of the future extension of the investigation campaign, a statistical analysis was performed for facilitating the possible discrimination of different cases and the related classification. Figure 9 shows the mean values (solid lines) and the standard deviation (bars) of the complex permittivity calculated from all the measurements of each of the four tissue groups (moles, healthy skin, malignant tissues and benign tissues).

As a general trend it is observed that the higher the complex permittivity, the higher the probability that the tissue is not a tumour. Conversely, for dielectric permittivity values lower than those corresponding to the adjacent normal skin, it is necessary a further assessment for discriminating between malignant and benign tumours. In addition, to identify similarities among the considered tissues of the 11 volunteers, the Principal Component Analysis (PCA) was carried out on the extrapolated dielectric parameters of the examined tissues. The goal is to extract significant information from the data and to present a final classification [57]. This analysis in fact, is typically used for dimensionality reduction by projecting each data point onto only the first few principal components to obtain lower-dimensional data, losing only little information. The PCA is also useful in order to identify clusters of elements: the higher is the distance between clusters, the more distinguishable is the data included in the clusters. Figure 10 shows the final result as deriving from the simultaneous processing of both real and imaginary permittivity data.

As expected, four main characteristics clusters can be observed, in which the four categorised typologies of cases are included. Particularly, considering that moles and healthy skin correspond both to normal conditions, their cumulative cluster area is positioned in the rightest portion the graph. On the other hand, lesions originating

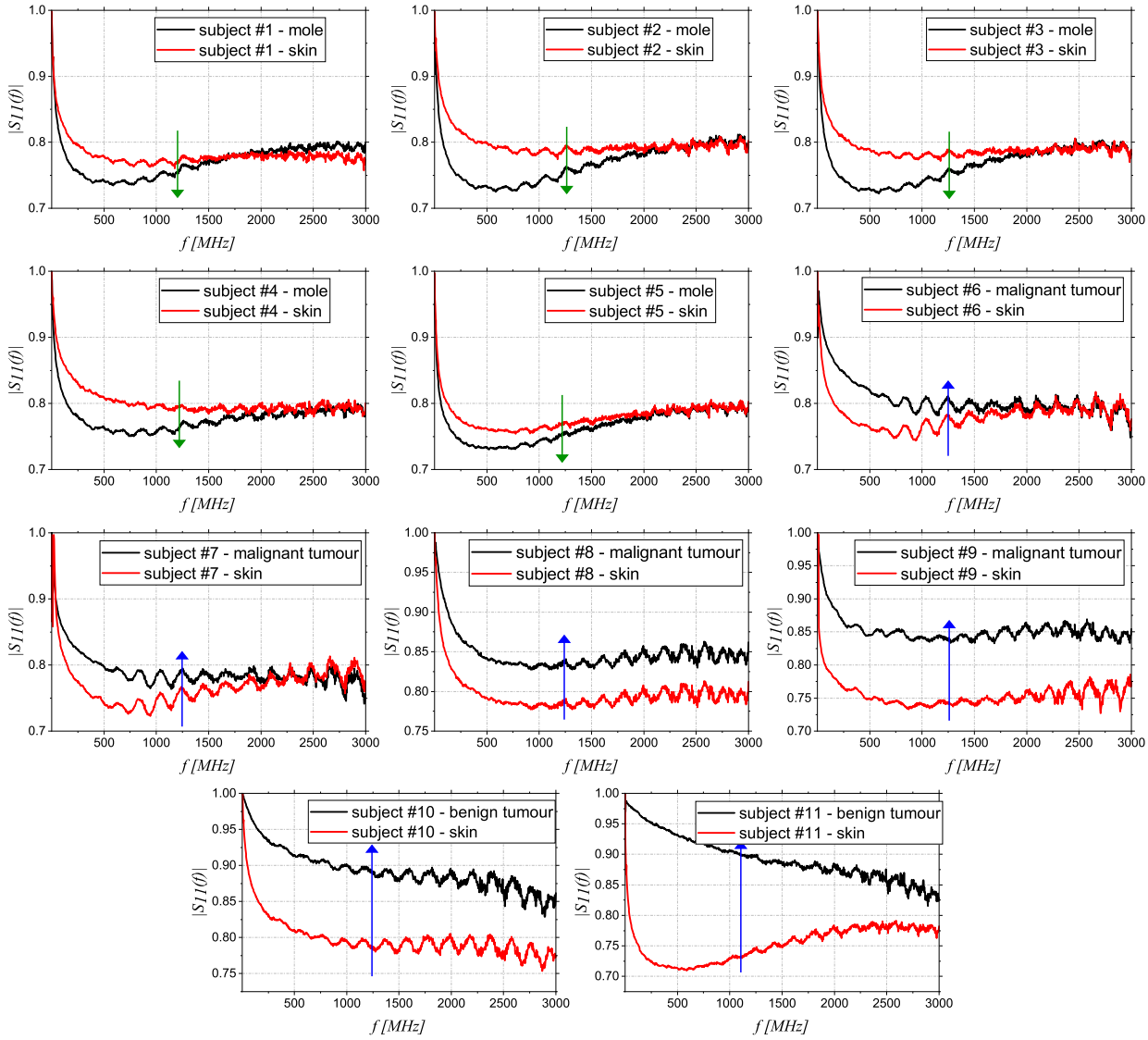

Figure 7. Magnitude of the $S_{11}(f)$ measured with the experimental setup on the 11 subjects as categorised: moles, malignant and benign tumours. For each test-case the comparison between lesion and normal skin is reported

by tumours both malignant and benign are displayed in the left part of the graph. Although a definitive and high accurate cluster classification would require a bigger dataset, these results indicate that the method is a suitable for discriminating among different cases thus anticipating that it is a good candidate for clinical support in the early cancer diagnostics.

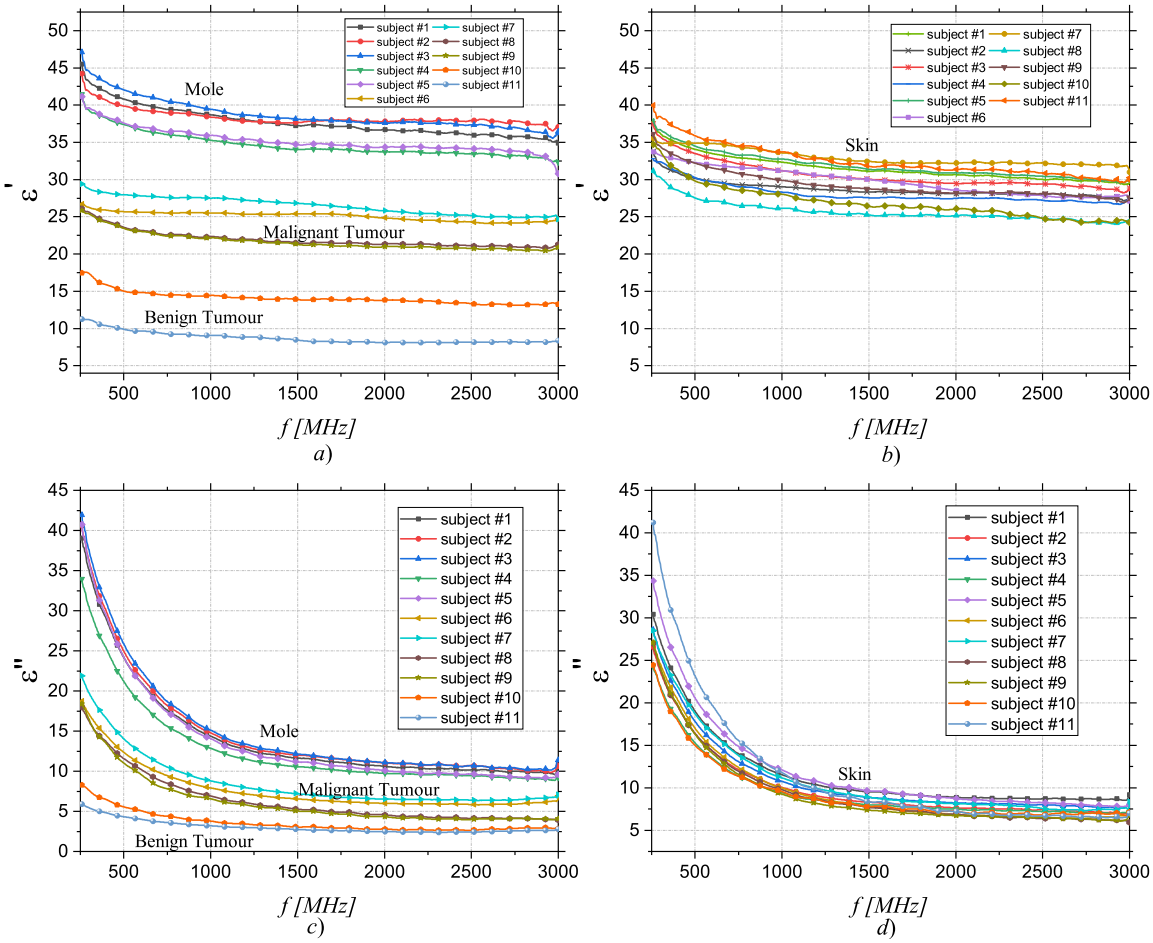

Figure 8. Comparative results of the complex permittivity obtained for each considered test-case: Real part of the dielectric permittivity for lesions **a)** and skin **b)**. Imaginary part of the dielectric permittivity for lesions **c)** and skin **d)**.

5 Conclusions

In this paper, a novel microwave reflectometry -based system for in-vivo skin cancer diagnosis is proposed and experimentally validated. This system potentially offers an attractive solution for non-invasive and in-vivo monitoring, in order to assess early-stage cancer diagnoses and favour prevention for several people with risk factors. The theoretical principle behind the proposed system exploits the significant different dielectric behaviour between healthy and pathological tissues, such as skin cancer. In particular, through the use of a miniaturized VNA and a specifically-designed open-ended coaxial probe, reflectometric measurements can be performed and then correlated to the frequency-dependent complex permittivity via a tailored data processing. The resulting contrast in complex permittivity between normal and tumoral tissues demonstrates the potential of the system for tissue classification and diagnosis, ensuring simultaneously low cost, compactness, comfortability and high sensitivity. The results of this paper can be used as a basis for taking further steps in skin cancer research. In this regard, future work will be dedicated to validate and to further test the proposed system on a large-scale campaign. Furthermore, in view of the practical application, the system will be improved through the integration of a Bluetooth interface and of a wearable flexible structure in order to allow the use also for periodic remote control and clinical monitoring on suspicious or surgically treated areas.

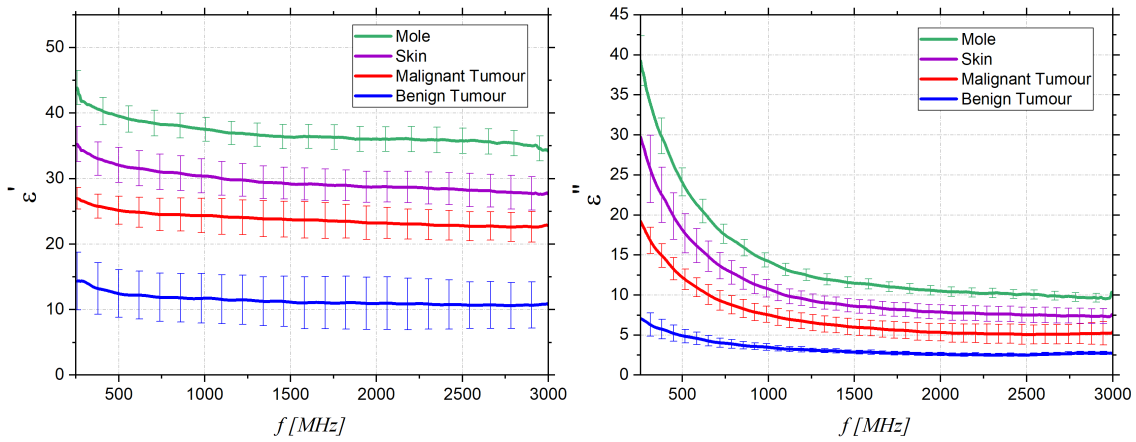

Figure 9. Complex permittivity of the five groups of tissues. The lines represent the mean values and the bars the standard deviation. Real part of complex permittivity (ε') **a)** and Imaginary part of complex permittivity (ε'') **b)**

Data availability

The datasets generated during and/or analysed during the current study are available from Gennaro Maietta on reasonable request sent to gmaietta2001@yahoo.it.

Author contributions statement

Conceptualization, A.C.,; methodology, R.S. and A.C.; investigation R.S., A.C., G.M. and E.F.; validation, R.S. and A.C.; formal analysis, R.S. and A.C.; data curation, R.S.; writing—original draft preparation, R.S; writing—review and editing, R.S. and A.C.; visualization, R.S. and A.C.; supervision, A.C. All authors have read and agreed to the published version of the manuscript.

Conflicts of Interest

The author(s) declare no competing interests.

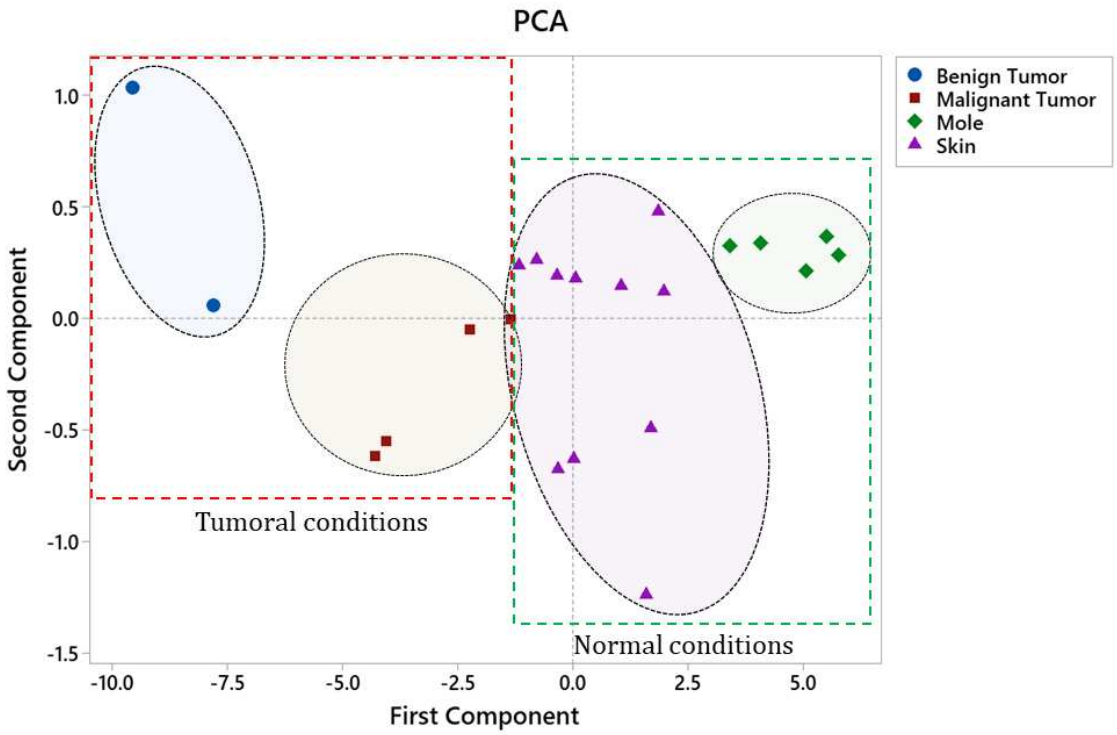

Figure 10. Final result of the PCA analysis conducted on the considered test-cases

References

1. Skin cancer foundation a 501(c)(3) nonprofit organization, skin cancer facts statistics (2022).

2. Swann, G. The skin is the body's largest organ. *J. Vis. Commun. Med.* **33(4)**, 148–149 (2010).

3. Tampa, M. *et al.* Recent advances in signaling pathways comprehension as carcinogenesis triggers in basal cell carcinoma. *J. Clin. Med.* **9(9)**, 3010 (2020).

4. Cohen, P. & Calame, A. Multiple skin neoplasms at one site (musk in a nest): A comprehensive review of basal cell carcinoma and benign or malignant "collision" tumors at the same cutaneous location. *Clin. Cosmet. Investig. Dermatol.* **13**, 731–741 (2020).

5. A.G., M. Basal cell carcinoma: pathogenesis, epidemiology, clinical features, diagnosis, histopathology, and management. *Yale J. Biol. Med.* **88(2)**, 167–179 (2015).

6. Alam, M. & Ratner, D. Cutaneous squamous-cell carcinoma. *N. Engl. J. Med.* **344**, 975–983 (2001).

7. Johnson, T., Rowe, D., Nelson, B. & Swanson, N. Squamous cell carcinoma of the skin (excluding lip and oral mucosa). *J. Am. Acad. Dermatol.* **26(3)**, 467–484 (1992).

8. Massone, C., Di Stefani, A. & Soyer, H. Dermoscopy for skin cancer detection. *Curr. Opin. Oncol.* **17(2)**, 147–153 (2005).

9. Nault, A., Zhang, C., Kim, K., Saha, S. & Bennett, Y., D.D.and Xu. Biopsy use in skin cancer diagnosis: Comparing dermatology physicians and advanced practice professionals. *JAMA Dermatol.* **151(8)**, 899–902 (2015).

10. MacFarlane, D. & Rapini, R. Biopsy techniques and interpretation. in: Macfarlane d.f. (eds) skin cancer management. *Springer* (2009).

11. Arpaia, P., De Benedetto, E. & Duraccio, L. Design, implementation, and metrological characterization of a wearable, integrated ar-bci hands-free system for health 4.0 monitoring. *Measurement* **177** (2021).

12. Arpaia, P., De Benedetto, E., Dodaro, C., Duraccio, L. & Servillo, G. Metrology-based design of a wearable augmented reality system for monitoring patient's vitals in real time. *IEEE Sensors J.* **21**, 11176–11183 (2021).

13. Zhang, J., Fan, Y., Song, Y. & Xu, J. Accuracy of raman spectroscopy for differentiating skin cancer from normal tissue. *Medicine (Baltimore)* **97(34)**, e12022 (2018).

14. Spreinat, A., Selvaggio, G., Erpenbeck, L. & Kruss, S. Multispectral near infrared absorption imaging for histology of skin cancer. *J. Biophotonics* **13(1)**, e201960080 (2020).

15. Li, D. *et al.* Detecting melanoma with a terahertz spectroscopy imaging technique. *Spectrochimica Acta Part A: Mol. Biomol. Spectrosc.* **234**, 1386–1425 (2020).

16. Herman, C. The role of dynamic infrared imaging in melanoma diagnosis. *Expert. Rev. Dermatol.* **18(2)**, 177–184 (2013).

17. Zakharov, P., Dewarrat, F., Caduff, A. & Talary, M. The effect of blood content on the optical and dielectric skin properties. *Physiol. Meas.* **32**, 131–149 (2010).

18. Gniadecka, M. *et al.* Melanoma diagnosis by raman spectroscopy and neural networks: Structure alterations in proteins and lipids in intact cancer tissue. *J. Invest. Dermatol.* **122**, 443–449 (2004).

19. Mirbeik-Sabzevari, A., Ashinoff, R. & Tavassolian, N. Ultra-wideband millimeter-wave dielectric characteristics of freshly excised normal and malignant human skin tissues. *IEEE Trans. Biomed. Eng.* **65(6)**, 1320–1329 (2018).

20. Pickwell, E. *et al.* Simulating the response of terahertz radiation to basal cell carcinoma using ex vivo spectroscopy measurements. *J. Biomed. Opt.* **10(6)**, 064021 (2005).

21. Wallace, V. P. Terahertz pulsed spectroscopy of human basal cell carcinoma. *Appl. Spectrosc.* **60(10)**, 1127–1133 (2006).

22. Mayrovitz, H., Gildenberg, S., Spagna, P., Killpack, L. & Altman, D. Characterizing the tissue dielectric constant of skin basal cell cancer lesions. *Ski. Res Technol.* **24(4)**, 686–691 (2018).

23. Chren, M. *et al.* Recurrence after treatment of nonmelanoma skin cancer: A prospective cohort study. *Arch. Dermatol.* **147(5)**, 540–546 (2011).

24. De Gruijl, F. Skin cancer and solar uv radiation. *Eur. J. Cancer* **35(14)**, 2003–2009 (1999).

25. Halpern, A. & Altman, J. Genetic predisposition to skin cancer. *Curr. Opin. Oncol.* **11(2)**, 132–138 (1999).

26. Tsai, K. & Tsao, H. The genetics of skin cancer. *Am. J. Med. Genet.* **131C**, 82–92 (2004).

27. Brown, M., Sharpe, C., MacMillan, D. & McGovern, V. Genetic predisposition to melanoma and other skin cancers in australians. *Med. J. Aust.* **1**, 852–853 (1971).

28. Danaei, G., Vander Hoorn, S., Lopez, A., Murray, C. & Ezzati, M. Comparative risk assessment collaborating group (cancers). causes of cancer in the world: comparative risk assessment of nine behavioural and environmental risk factors. *Lancet* **366(9499)**, 1784–1793 (2005).

29. Gerstenblith, M., Shi, J. & Landi, M. Genome-wide association studies of pigmentation and skin cancer: a review and meta-analysis. *Pigment. Cell Melanoma Res.* **23**, 587–606 (2010).

30. Urbach, F. Geographic distribution of skin cancer. *J. Surg. Oncol.* **3**, 219–234 (1971).

31. Auerbach, H. Geographic variation in incidence of skin cancer in the united states. *Public Heal. Rep.* **76(4)**, 345–348 (1961).

32. Stern, R. The mysteries of geographic variability in nonmelanoma skin cancer incidence. *Arch. Dermatol.* **135(7)**, 843–844 (1999).

33. Rangwala, S. & Tsai, K. Roles of the immune system in skin cancer. *Br. J. Dermatol.* **165**, 953–965 (2011).

34. Harwood, C. A. & Proby, C. M. Human papillomaviruses and non-melanoma skin cancer, current opinion in infectious diseases. *Curr. Opin. Infect. Dis.* **15(2)**, 101–114 (2002).

35. Nindl, I. & Rösl, F. Molecular concepts of virus infections causing skin cancer in organ transplant recipients. *Am. J. Transpl.* **8(11)**, 2199–2204 (2008).

36. Rigel, D., Friedman, R., Kopf, A. & Polsky, D. Abcde—an evolving concept in the early detection of melanoma. *Arch. Dermatol.* **141(8)**, 1032–1034 (2005).

37. Robinson, J. & Ortiz, S. Use of photographs illustrating abcde criteria in skin self-examination. *Arch. Dermatol.* **145(3)**, 332–333 (2009).

38. Giaquinto, N. *et al.* Criteria for automated estimation of time of flight in tdr analysis. *IEEE Trans. Instrum. Meas.* **65(5)**, 1215–1224 (2016).

39. Cataldo, A., De Benedetto, E., Cannazza, G., Piuzzi, E. & Giaquinto, N. Embedded tdr wire-like sensing elements for monitoring applications. *Measurement* **68**, 236–245 (2015).

40. Cataldo, A., De Benedetto, E., Cannazza, G., Piuzzi, E. & Pittella, E. Tdr-based measurements of water content in construction materials for in-the-field use and calibration. *IEEE Trans. Instrum. Meas.* **67(5)**, 1230–1237 (2018).

41. Piuzzi, E. *et al.* A comparative assessment of microwave-based methods for moisture content characterization in stone materials. *Measurement* **114**, 493–500 (2018).

42. Schiavoni, R. *et al.* Feasibility of a wearable reflectometric system for sensing skin hydration. *Sensors* **20(10)**, 2833 (2020).

43. Cataldo, A., De Benedetto, E., Masciullo, A. & Cannazza, G. A new measurement algorithm for tdr-based localization of large dielectric permittivity variations in long-distance cable systems. *Measurement* **174**, 109066 (2021).

44. Cataldo, A., De Benedetto, E., Angrisani, L., Cannazza, G. & Piuzzi, E. A microwave measuring system for detecting and localizing anomalies in metallic pipelines. *IEEE Trans. Instrum. Meas.* **70**, 1–11 (2021).

45. Cataldo, A. *et al.* Microwave reflectometric systems and monitoring apparatus for diffused-sensing applications. *Acta Imeko* **10(3)** (2021).

46. Mehta, P. *et al.* Microwave reflectometry as a novel diagnostic tool for detection of skin cancers. *IEEE Trans. Instrum. Meas.* **55(4)**, 1309–1316 (2016).

47. Gniadecka, M., Nielsen, O. & Wulf, H. Water content and structure in malignant and benign skin tumours. *J. Mol. Struct.* **661**, 405–410 (2003).

48. Gniadecka, M. *et al.* Melanoma diagnosis by raman spectroscopy and neural networks: Structure alterations in proteins and lipids in intact cancer tissue. *J. Investig. Dermatol.* **122(2)**, 443–449 (2004).

49. Gabriel, C., Gabriel, S. & Corthout, E. The dielectric properties of biological tissues: I. literature survey. *Phys. Med. Biol.* **41(11)** (1996).

50. Said, T. & Varadan, V. Variation of cole-cole model parameters with the complex permittivity of biological tissues. *IEEE MTT-S Int. Microw. Symp. Dig.* 1445–1448 (2009).

51. Gabriel, S., Lau, R. & Gabriel, C. The dielectric properties of biological tissues: III. parametric models for the dielectric spectrum of tissues. *Phys. Med. Biol.* **41(11)**, 2271–2293 (1996).

52. Wei, S. & Sridhar, S. Radiation-corrected open-ended coax line technique for dielectric measurements of liquids up to 20 ghz. *IEEE Trans. Microw. Theory Tech.* **39(3)**, 526–531 (1991).

53. Gabriel, C. Compilation of the dielectric properties of body tissues at rf and microwave frequencies. (1996).

54. Peckham, M., Knibbs, A. & Paxton, S. Skin functions and layers.

55. World medical association, world medical association declaration of helsinki: Ethical principles for medical research involving human subjects. *JAMA* **310(20)**, 2191–2194 (2013).

56. Piuzzi, E. *et al.* A comparative analysis between customized and commercial systems for complex permittivity measurements on liquid samples at microwave frequencies. *IEEE Trans. Instrum. Meas.* **62(5)**, 1034–1046 (2013).

57. Jolliffe, I. Principal component analysis, in: Everitt, b. s. and howell, d. c. (eds.). *Encycl. statistics behavioral science* **John Wiley and Sons Ltd, New York**, 1580 –1584.

Supplementary Files

This is a list of supplementary files associated with this preprint. Click to download.

- RawData.xlsx